

Bazı Saf Metaller İçin 59.5 Kev Fotonlar Kullanılarak $24 \leq Z \leq 56$ Atom Numarası Aralığında K-L Tabakası Boşluk Geçiş Olasılıkları

Selim Kaya^{1*}, Salih Mustafa Karabıdak¹, Uğur Çevik²

¹Gümüşhane Üniversitesi, Mühendislik ve Doğa Bilimleri Fakültesi, Fizik Mühendisliği,
Gümüşhane

²Karadeniz Teknik Üniversitesi, Fen Fakültesi, Fizik Bölümü, Trabzon,

selimkaya@gumushane.edu.tr

ÖZET

K-L tabakası için boşluk geçiş olasılığı (η_{KL}) Cr, Fe, Co, Cu, Zn, Ga, Se, Y, Mo, Cd, In, Sn, Te ve Ba gibi bazı saf metaller için $I_{K\beta}/I_{K\alpha}$ şiddet oranı ölçümlerinden elde edildi. Hedef metaller 59,5 keV'lik gama ışınları yayınlayan 50 mCi'lik ²⁴¹Am radyoaktif kaynak tarafından uyarıldı. Numunelerden yayınlanan karakteristik K X-ışınları 5,96 keV'de 0,150 keV'lik ayırma gücüne sahip süper Si(Li) detektör kullanılarak belirlendi. Elde edilen deneysel K-L tabakası boşluk geçiş olasılık değerleri ile teorik değerler ile karşılaştırıldı. Ölçülen değerlerin teorik değerlerle uyum içinde olduğu gözlemlendi.

Anahtar Kelimeler: Boşluk geçiş olasılığı, EDXRF; Süper Si (Li) Detektör

K-L Vacancy Transfer Probabilities For Some Pure Metals In The Atomic Range $24 \leq Z \leq 56$ Using 59.5 Kev Photons

ABSTRACT

The probabilities for vacancy transfer from K to L shell (η_{KL}) for some pure metals such as Cr, Fe, Co, Cu, Zn, Ga, Se, Y, Mo, Cd, In, Sn, Te and Ba were obtained by measuring the $I_{K\beta}/I_{K\alpha}$ intensity ratios. The targets were irradiated with γ -photons at 59.5 keV from 50 mCi ²⁴¹Am radioactive source. The characteristic K X-rays emitted by samples were detected by using a super Si(Li) detector having a resolution of 150 eV at 5,96 keV. The obtained experimental values of vacancy transfer probabilities from K to L shell have been compared with theoretical values. The measured values were in good agreement with theoretical values.

Keywords: Vacancy transfer probability, EDXRF, Super Si(Li) Detector

1. Introduction

X-ray fluorescence (XRF) spectrometry is used worldwide. The most established technique is energy dispersive X-ray fluorescence (EDXRF) for quantitative analysis because EDXRF is relatively inexpensive and requires less technical effort to run the system. EDXRF is very useful for determination XRF parameters such as production cross sections, fluorescence yields, intensity ratios and vacancy transfer probabilities. Accurate values of these parameters are required in several fields such as atomic, molecular and radiation physics, material science, environmental science, agriculture, forensic science, dosimetric computations for health physics, cancer therapy, elemental analysis, basic studies of nuclear physics, etc.

The creation of a vacancy in an atomic shell initiates a series of rearrangement process which may become quite complicated. A single vacancy created by photons, electrons or charged-particles of sufficient energy is rapidly filled up by an electron coming from some higher shell or sub-shell. The difference in the binding energy between the two shells (e.g., the K-L2 energy difference) either is released as a K X-ray photon or is transferred to another bound electron which is ejected. This results in an atom with two vacancies. Continuation of this process gives rise to the emission L, M, N, etc. X-rays and Auger electrons, resulting in an atom with multiple vacancies in its outermost shells; i.e., a highly charged ion. The radiative transitions can be adequately explained in terms of multipole theory which predicts that by far the most important mode is the electric dipole. The nonradiative or Auger transitions occur because of Coulomb interaction existing among different electrons in the atom [1].

The measurement of K_{β} / K_{α} intensity ratios is important because of comparison with theoretical predictions based on atomic model. While the K_{α} X-rays is arising arise from transitions from the L- to the K-shell, the K_{β} X-rays arise from transitions from the M-, N-, O-, etc. to the K-shell The X-ray intensity ratio $I_{K\beta}/I_{K\alpha}$ has been extensively studied in recent years. It is the ratio of the radiative transition probabilities when a K vacancy is filled from the M, N, O, etc.

Rao et al. showed that the K_{β} / K_{α} intensity ratios depend on the excitation in 3d elements but they could not find such dependence for the high Z elements [2]. Dhal and Padhi have investigated relative K X-ray intensities on the elements from Mn to Sb using 59.5 keV γ -rays [3]. Similarly, Ertugrul have measured K_{β} / K_{α} intensity ratios in element range $22 \leq Z \leq 69$ at 59.5 keV [4]. Ertugrul and Simsek have measured K X-ray relative intensity of some high Z elements [5]

In the earlier measurements [6–8], the authors used two radioisotope sources for excitation of targets. The method is based on the number of L X-rays produced at the photon excitation energy below the K edge and at the excitation energy above the K edge, where the major contribution to L shell vacancies comes from the decay K shell vacancies. Ertugrul [9,10] has measured total, radiative and radiationless vacancy transfer probabilities from K to Li subshell for some elements in the mean atomic number region. Öz [11] determined the ratios of emission probabilities of Auger electrons and K-L shell radiative vacancy transfer probabilities for 17 elements from Mn to Mo. Besides, Ertugrul et al. [12] calculated vacancy transfer probabilities from K to L in the atomic region $23 \leq Z \leq 57$.

The main purpose of this study is to determine the vacancy transfer probabilities K to L using these $I_{K\beta}/I_{K\alpha}$ intensity ratios for some pure metals in the atomic range $24 \leq Z \leq 56$

2. Experimental Arrangement

The Geometry of the experimental setup used in the measurements are shown schematically in Fig. 1. Excited pure metals were supplied commercially by Aldrich and Alfa Aesar. The purity of the samples of Cr, Fe, Co, Cu, Zn, Ga, Se, Y, Mo, Cd, In, Sn, Te, Ba, with thickness of 108 mg.cm^{-2} have been used for the measurement was 99.99%.. The samples were irradiated by 59.5 keV photons emitted by an annular 50 mCi ^{241}Am .

The samples were placed at 45° angles with respect to the beam from the source and fluorescent X-rays emitted 90° to the source were detected by a Si(Li) detector. The K X-ray spectra from pure metals were detected and analyzed with a super Si(Li) detector (FWHM=150 eV at 5.9 keV) manufactured by Canberra with an active area of 30 mm^2 , thickness 3 mm and Be window thickness 25 μm .

The output from the preamplifier, with pulse pile-up rejection capability, was fed to a multi-channel analyzer interfaced with a personal computer provided with suitable software (Genie 2000) for data acquisition and peak analysis program (Genie 2000). The live time was selected to be 5000 s for all elements. The peak areas have been obtained from the spectrum obtained for each measurement. The selected K X-ray spectrum of Ba is shown in Fig. 2.

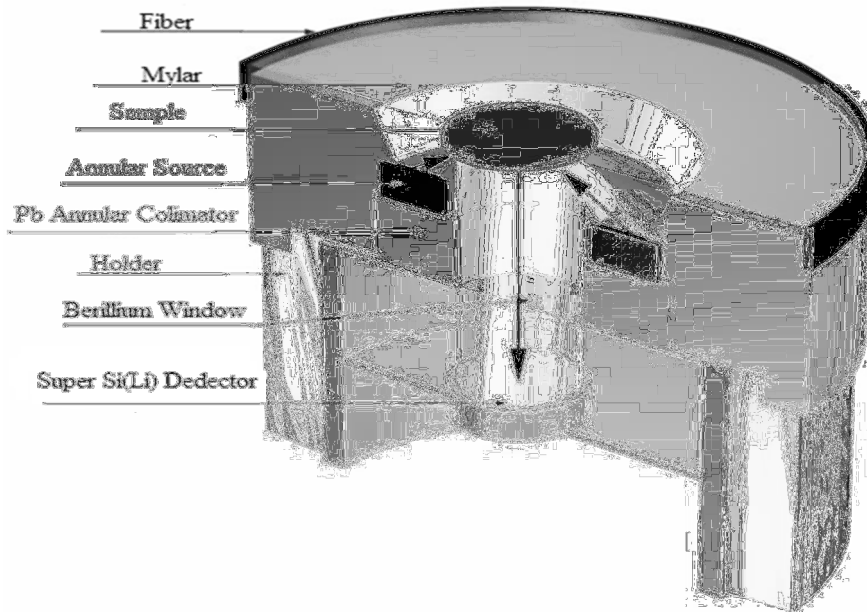


Fig. 1. Experimental setup.

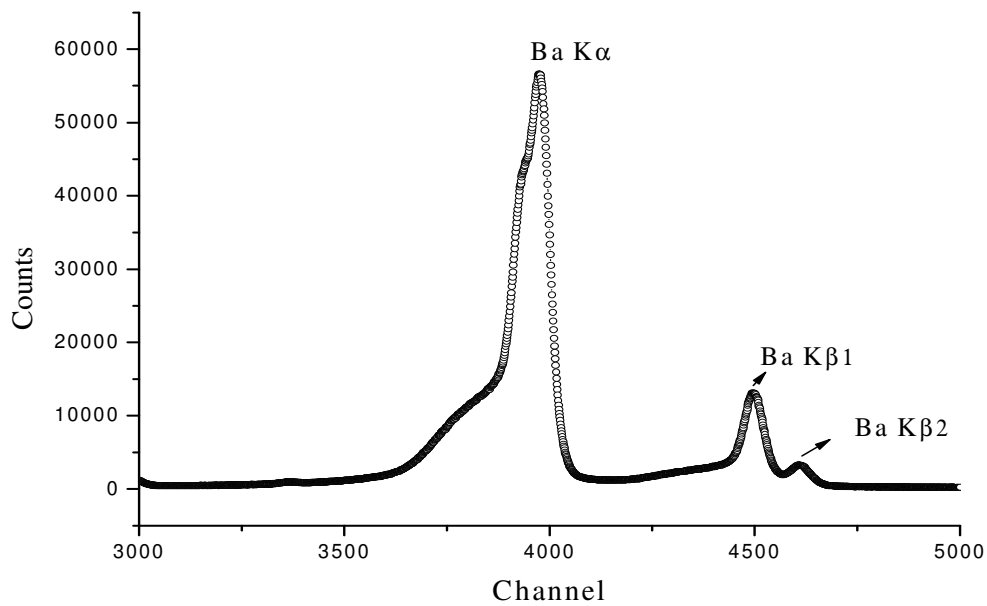


Fig. 2. Typical K X-ray spectrum for Ba

2.1. Calculation of the experimental k to l shell vacancy transfer probabilities and $I_{K\beta}/I_{K\alpha}$ intensity ratios)

Our experimental K to L shell vacancy transfer probabilities, η_{KL} were obtained using the following relation [13]:

$$\eta_{KL} = \frac{2 - \omega_K}{1 + (I_{K\beta}/I_{K\alpha})} \quad (1)$$

where ω_K is the fluorescence yield and $I_{K\beta}/I_{K\alpha}$ is intensity ratio of K X-rays. The ratio of the intensity of the characteristic X-ray $I_{K\beta}/I_{K\alpha}$ have been calculated using the following relation,

$$\frac{I_{K\beta}}{I_{K\alpha}} = \frac{N_{K\beta} \beta_{K\alpha} \epsilon_{K\alpha}}{N_{K\alpha} \beta_{K\beta} \epsilon_{K\beta}} \quad (2)$$

where $N_{K\alpha}$ and $N_{K\beta}$ are the net counts observed under the peaks corresponding to K_α and K_β X-rays, respectively. $\epsilon_{K\alpha}$ and $\epsilon_{K\beta}$ are the efficiencies of the detector for the K_α and K_β series of x-rays. $\beta_{K\alpha}$ and $\beta_{K\beta}$ are the target self-absorption correction factors for incident and emitted radiation.

The peak areas were determined after the K_α and K_β photo peak areas were separated by fitting the measured spectra with multi-Gaussian function plus polynomial backgrounds using Microcal Origin 8.0 software program.

The values of the self-absorption correction factor β were calculated from following equation [14]:

$$\beta = \frac{1 - \exp[-(\mu_{inc} \sec \theta_1 + \mu_{emt} \sec \theta_2) t]}{(\mu_{inc} \sec \theta_1 + \mu_{emt} \sec \theta_2) t} \quad (3)$$

where μ_{inc} (cm^2g^{-1}) and μ_{emt} (cm^2g^{-1}) are the mass absorption coefficients [15] at the incident photon energy and fluorescent x-ray energy of sample, respectively, and t ($\text{g}\cdot\text{cm}^{-2}$) is the measured thickness of sample and θ_1 and θ_2 are the angles of incident photons and emitted x-ray with respect to the normal of the sample surface, respectively.

3. Theoretical Calculations

The vacancy transfer probabilities from K to L shell is obtained as the number of L_i subshell vacancies produced in the decay of one K shell vacancy through radiate K- L_i transitions or through Auger K- L_iL_j and K- L_iX ($X=M,N,O,\dots$) transitions. The average number of η_{KL_i} ;

$$\eta_{KL_i} = \eta_{KL_i}(R) + \eta_{KL_i}(A) \quad (4)$$

Where $\eta_{KL_i}(R)$ and $\eta_{KL_i}(A)$ are the radiative and auger transition probabilities of the K to L_i subshell, respectively. The number of $\eta_{KL_i}(R)$ is the proportional to the probability that a K- L_i radiative transition takes place:

$$\eta_{KL_i}(R) = w_K [I(KL_i) / I_K(R)] \quad (5)$$

where, $I(KL_i)$ is the K- L_i X-ray intensity and $I_K(R)$ is the total intensity of the K X-rays.

The η_{KL_i} was calculated using the following equations [18],

$$\eta_{KL_1} = \frac{1}{\Gamma(K)} [\Gamma_R(KL_1) + 2\Gamma_A(KL_1KL_1) + \Gamma_A(KL_1KL_2) + \Gamma_A(KL_1KL_3) + \Gamma_A(KL_1X)] \quad (6)$$

$$\eta_{KL_2} = \frac{1}{\Gamma(K)} [\Gamma_R(KL_2) + 2\Gamma_A(KL_2KL_2) + \Gamma_A(KL_2KL_3) + \Gamma_A(KL_2X)] \quad (7)$$

$$\eta_{KL_3} = \frac{1}{\Gamma(K)} [\Gamma_R(KL_3) + 2\Gamma_A(KL_3KL_3) + \Gamma_A(KL_3KL_3) + \Gamma_A(KL_3X)] (X = M, N, O, \text{etc.}) \quad (8)$$

In these equations, Γ_R and Γ_A are the radiative and the Auger partial widths corresponding to the transitions between the shells written in the parenthesis, and Γ is the total level width. The radiative and Auger transition rates were tabulated by Scofield [19] and Chen et al. [20], respectively.

4. Results And Discussion

The calculated values of the K to L shell vacancy transfer probability, η_{KL} and intensity ratio $I_{K\beta}/I_{K\alpha}$ for some pure metals of medium atomic numbers listed in Table 1 and Table 2 with the theoretical and other experimental values. The uncertainties in the values of the K to L shell vacancy transfer are estimated to be ranged from 2% to 7%. These uncertainties are sum of the several errors caused by the area evaluation under the K_α and K_β X-ray peak (2%), in the absorption correction factor ratio (3%), the product I_0G_e (4–6%) and the other systematic errors (2–4%).

Our experimental values of the $I_{K\beta}/I_{K\alpha}$ intensity ratios and theoretical values are plotted as a function of the atomic number in the Fig 3. Similarly; our Experimental results of the K to L shell total vacancy transfer probabilities are plotted as a function of the atomic number. The unknown experimental values were approximated in the medium atomic number by fitting the multiple-order polynomial by using known experimental values and these fitted values are listed in Table 2. The fitted polynomial is shown in Fig. 4.

Table 1. Experimental $K\beta/K\alpha$ intensity ratios for some pure metals are compared with the most probable experimental values Hansen, with theoretical values of Scofield and Khan.

Element	Z	Experimental	Scofield [16]	Khan [17]	Fitted values
Cr	24	0.132±0.005	0.136	0.133	0.123
Fe	26	0.135±0.007	0.139	0.134	0.131
Co	27	0.137±0.008	----	0.135	0.135
Cu	29	0.136±0.005	0.138	0.137	0.144
Zn	30	0.136±0.005	0.141	0.139	0.147
Ga	31	0.143±0.006	----	----	0.152
Se	34	0.167±0.006	0.162	0.161	0.164
Y	39	0.191±0.007	----	----	0.183
Mo	42	0.197±0.006	0.198	0.195	0.194
Cd	48	0.212±0.007	----	0.216	0.213
In	49	0.219±0.008	----	0.218	0.216
Sn	50	0.221±0.009	0.223	0.222	0.220
Te	52	0.226±0.009	----	0.227	0.226
Ba	56	0.238±0.010	0.243	0.237	0.237

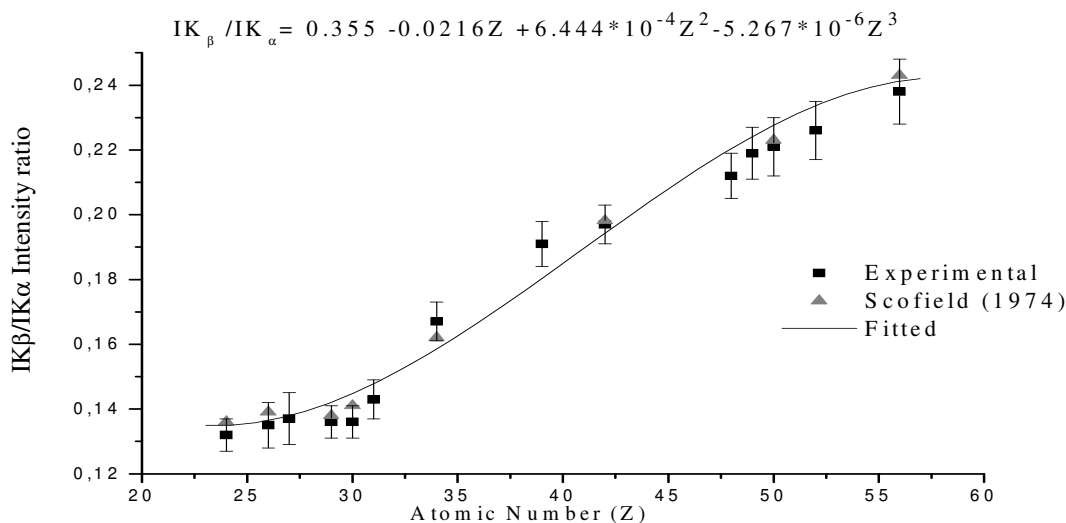


Fig 3. Experimental, theoretical and fitted $I_{K\beta} / I_{K\alpha}$ intensity ratio values some pure metals values as a function of atomic number.

Table 2. Our experimental results K to L shell vacancy transfer probabilities for some pure metals compared theoretical values

Element	Z	Experimental	Fitted	η_{KL}	T ^a	T ^b	Theoretical
Cr	24	1,523±0,044	1,507		1,495	1,508	1,515
Fe	26	1,463±0,042	1,466		1,439	1,447	1,448
Co	27	1,431±0,041	1,436		--	1,418	1,416
Cu	29	1,372±0,041	1,363		--	1,357	1,354
Zn	30	1,343±0,040	1,336		1,316	1,326	1,324
Ga	31	1,305±0,038	1,305		--	1,294	1,295
Se	34	1,208±0,036	1,208		1,200	1,202	1,215
Y	39	1,083±0,037	1,086		--	1,081	1,101
Mo	42	1,031±0,041	1,033		1,030	1,029	1,045
Cd	48	0,954±0,038	0,954		0,952	0,953	0,958
In	49	0,941±0,028	0,942		--	0,944	0,947
Sn	50	0,926±0,037	0,934		0,932	0,934	0,937
Te	52	0,913±0,046	0,917		0,914	0,917	0,918
Ba	56	0,886±0,026	0,885		0,887	0,888	0,888

T^a Rao et al.

T^b Schönfeld et al

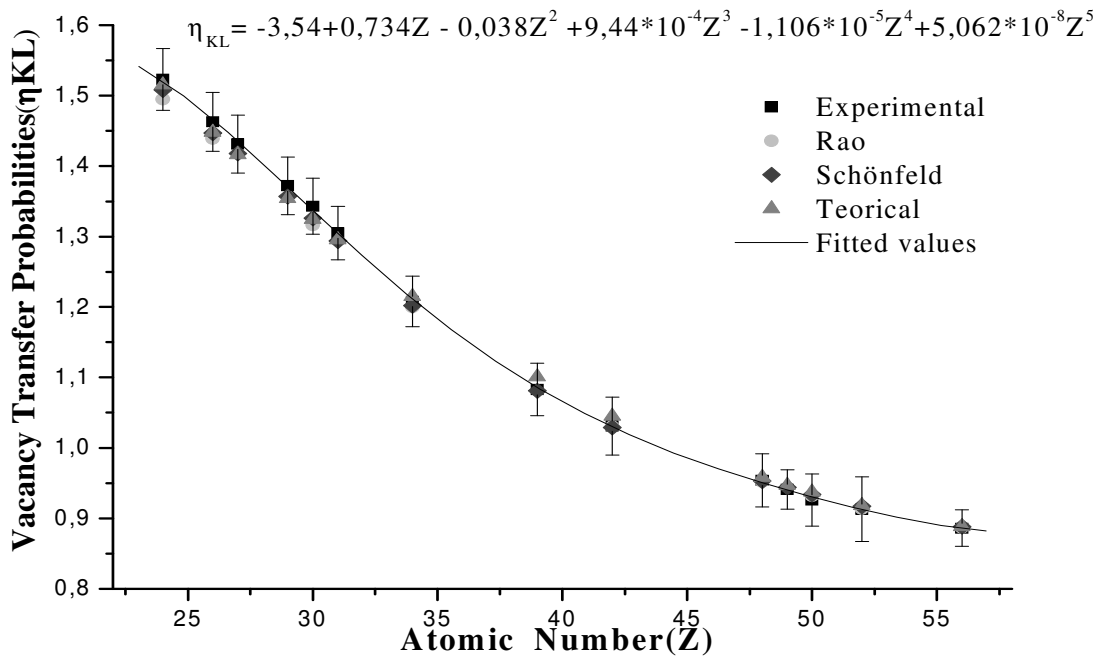


Fig 4. Experimental, theoretical and fitted K to L shell vacancy transfer probabilities values as a function of atomic number.

In order to facilitate a better and closer comparison between theory and experiment the results are presented in the graphical form as shown in Fig. 4. It is clearly seen from this figure then experimental results are in good agreement with the theoretical values for the K to L shell vacancy transfer probabilities in the medium atomic number.

Consequently, the agreement between the experimental results and the theoretical values leads to the conclusion that the present method will be beneficial for determining intensity ratios and. vacancy transfer probabilities. Thus, the obtained data can be helpful for radioisotope XRF method for elemental analysis.

REFERENCES

- [1] Fink R W, Jopson RC, Mark H, Swift C D, Rev Mod Phys 38 3 (1989).
- [2] Rao V N, Reddy S B, Satyanarayana G and Sastry D L , Physica B and C 143 375 (1986)
- [3] Dhal B B, Padhi H C, Phys. Rev. A 50 1096 (1994).

- [4] Ertugrul M, Sögüt Ö, Simsek Ö and Büyükkasap E J, Phys. B 34 909 (2001).
- [5] Ertugrul M and Simsek Ö, J. Phys. B 35 601 (2002).
- [6] Puri S, Mehta D, Chand B, Singh N, Trehan P N, Nucl Instrum Methods B 73 443 (1993).
- [7] Puri S, Mehta D, Chand B, Singh N, Trehan P N, Nucl Instrum Methods B 74 347 (1993).
- [8] Ertugrul M, Dogan O, Şimşek Ö, Turgut Ü, Phys Rev A 55 303 (1997).
- [9] Ertugrul M, J Anal Atom Spectrum 17 64 (2002).
- [10] Ertugrul M., Spectrochim Acta B 57 63 (2002).
- [11] E. Öz, Journal of Quantitative Spectroscopy & Radiative Transfer 97 41 (2006).
- [12] B. Ertuğral, G. Apaydın, A. Tekbıyık, E. Tırasoğlu, U. Çevik, A.I. Kobya and M. Ertuğrul, *Eur. Phys. J. D.* 37 371 (2006).
- [13] E. Schönfeld, H. Janben, Nucl. Instrum. Methods A 369 527 (1996)
- [14] L. F. S. Coelho, M. B. Gaspar, J. Eichler, Phys. Rev. A. 40(7), 4093 (1989).
- [15] J. H. Hubbell, S. M. Seltzer, National Institute of Standards and Technology Center for Radiation Research, Document No: NISTIR 5632 (1995).
- [16] Scofield J H Atom. Data Nucl. Data Tables 14 121 (1974)
- [17] Khan M R and Karimi M X-Ray Spectrom 9 32 (1980).
- [18] V.P. Rao, M.H. Chen, B. Crasemann, Phys. Rev., A 5 997 (1972)
- [19] J.H. Scofield, Atom Data Tables 14 121 (1974)
- [20] M.H. Chen, B. Crasemann, H. Mark, At. Data Nucl. Data Tables 24 13 (1979)